Organic Geochemistry 78 (2015) 99–109

Contents lists available at ScienceDirect

Organic Geochemistry

journal homepage: www.elsevier.com/locate/orggeochem

Effect of aridity on $\delta^{13}C$ and δD values of C_3 plant- and C_4 graminoid-derived leaf wax lipids from soils along an environmental gradient in Cameroon (Western Central Africa)

Valérie F. Schwab [a,*], Yannick Garcin [b], Dirk Sachse [b], Gilbert Todou [c], Olivier Séné [c], Jean-Michel Onana [d], Gaston Achoundong [d], Gerd Gleixner [a]

[a] Max-Planck-Institut für Biogeochemie, Jena, Germany
[b] DFG-Leibniz Center for Surface Process and Climate Studies, Institut für Erd- und Umweltwissenschaften, Universität Potsdam, Germany
[c] Faculté des Sciences, University of Maroua, Cameroon
[d] National Herbarium of Cameroon, IRAD, Yaoundé, Cameroon

ARTICLE INFO

Article history:
Received 25 February 2014
Received in revised form 5 September 2014
Accepted 9 September 2014
Available online 2 October 2014

Keywords:
Evapotranspiration
D-enrichment
Pentacyclic triterpene methyl ethers
PTMEs
n-Alkane
Compound-specific isotope
Paleo
Climate
Proxy

ABSTRACT

The observation that the hydrogen isotope composition (δD) of leaf wax lipids is determined mainly by precipitation δD values, has resulted in the application of these biomarkers to reconstruct paleoclimate from geological records. However, because the δD values of leaf wax lipids are additionally affected by vegetation type and ecosystem evapotranspiration, paleoclimatic reconstruction remains at best semi-quantitative. Here, we used published results for the carbon isotope composition ($\delta^{13}C$) of *n*-alkanes in common plants along a latitudinal gradient in C_3/C_4 vegetation and relative humidity in Cameroon and demonstrated that pentacyclic triterpene methyl ethers (PTMEs) and *n*-C_{29} and *n*-C_{31} in the same soil, derived mainly from C_4 graminoids (e.g. grass) and C_3 plants (e.g. trees and shrubs), respectively. We found that the δD values of soil *n*-C_{27}, *n*-C_{29} and *n*-C_{31}, and PTMEs correlated significantly with surface water δD values, supporting previous observations that leaf wax lipid δD values are an effective proxy for reconstructing precipitation δD values even if plant types changed significantly. The apparent fractionation (ε_{app}) between leaf wax lipid and precipitation δD values remained relatively constant for C_3-derived long chain *n*-alkanes, whereas ε_{app} of C_4-derived PTMEs decreased by 20‰ along the latitudinal gradient encompassing a relative humidity range from 80% to 45%. Our results indicate that PTME δD values derived from C_4 graminoids may be a more reliable paleo-ecohydrological proxy for ecosystem evapotranspiration within tropical and sub-tropical Africa than *n*-alkane δD values, the latter being a better proxy for surface water δD values. We suggest that vegetation changes associated with different plant water sources and/or difference in timing of leaf wax synthesis between C_3 trees of the transitional class and C_3 shrubs of the savanna resulted in a D depletion in soil long chain *n*-alkanes, thereby counteracting the effect of evapotranspiration D enrichment along the gradient. In contrast, evaporative D enrichment of leaf and soil water was significant enough to be recorded in the δD values of PTMEs derived from C_4 graminoids, likely because PTMEs recorded the hydrogen isotopic composition of the same vegetation type.

1. Introduction

The observation that the hydrogen isotope composition (δD) of *n*-alkanes correlates with precipitation δD values over a large spatial scale (e.g. Sauer et al., 2001; Sachse et al., 2004, 2012; Garcin et al., 2012) has resulted in their widespread use for reconstructing past climate (e.g. Hou et al., 2008; Mügler et al., 2010; Sinninghe Damsté et al., 2011; Schefuss et al., 2011; Handley et al., 2012; Guenther et al., 2013). However, because *n*-alkane δD values can be additionally affected by secondary factors such as vegetation type (e.g. Krull et al., 2006; Sachse et al., 2012) or ecosystem evapotranspiration (e.g. Smith and Freeman, 2006; Sachse et al., 2010; Kahmen et al., 2013a,b), paleoclimatic reconstruction based on their integrated isotopic signal in geological records remains qualitative or semi-quantitative. By measuring the carbon isotope composition ($\delta^{13}C$) and δD values of lipids specifically derived from

* Corresponding author at: Friedrich Schiller University, Jena, Institute for Inorganic and Analytic Chemistry, Germany.
E-mail address: vf.schwab@uni-jena.de (V.F. Schwab).

http://dx.doi.org/10.1016/j.orggeochem.2014.09.007
0146-6380/

C_3 plants (e.g. trees or shrubs) and C_4 graminoids (e.g. grass) in soil from a latitudinal gradient in C_3/C_4 vegetation and aridity of Cameroon, we aimed to determine the reliability of lipid δD values as paleo-precipitation and ecosystem paleo-evapotranspiration proxies.

Plant water source δD value and subsequent evaporative D enrichment of leaf water mainly control leaf wax lipid δD value (e.g. Sachse et al., 2012; Kahmen et al., 2013a,b). Recently, it has been demonstrated that evaporative D enrichment of leaf water, which is expected to be greater under arid conditions, is linearly related to the D enrichment of *n*-alkanes in both C_3 trees and C_4 graminoids grown under controlled conditions in climate chambers (Kahmen et al., 2013a). These results allow quantifying the D enrichment of *n*-alkanes driven by leaf water evaporative D enrichment and thus might potentially be applied to contemporary plants as ecohydrological proxies for evapotranspiration (Kahmen et al., 2013b). It has been demonstrated that evaporative D enrichment of leaf water occurs to a lower extent in C_4 graminoids than in C_3 plants, resulting in cultured plants to lower *n*-alkane δD values (by 50‰) in C_4 graminoids than in C_3 plants (Kahmen et al., 2013a). However in arid ecosystems, water in the upper soil layers is commonly D-enriched relative to the water in deeper soil layers (e.g. Schulze, 1986; Dawson and Pate, 1995; Oliveira et al., 2005). Because shallow rooted C_4 graminoids (e.g. grass) typically access more D-enriched water than deeper rooted C_3 plants (e.g. trees or shrubs), stratification in soil water δD values might result alternatively in heavier *n*-alkanes in C_4 graminoids than in C_3 plants (Krull et al., 2006). Consequently, intrinsic factors related to different plant physiology between C_3 plants and C_4 graminoids may either increase or decrease the effects of aridity on their leaf wax lipid δD values (e.g. Bi et al., 2005; Chikaraishi and Naraoka, 2006, 2007; Smith and Freeman, 2006). Without better knowledge of the effect of these factors on the integrated plant lipid δD values in geological records, quantitative interpretations will remain limited.

Because isotope fractionation during carbon fixation differs between plant pathways, C_3 and C_4 plants differ in their carbon isotope composition (Farquhar et al., 1989). Commonly, C_3 plant-derived lipids exhibit $\delta^{13}C$ values of ca. −35‰ ± 5‰ and C_4 plant-derived lipids ca. −20‰ ± 2‰ (Chikaraishi et al., 2004; Rommerskirchen et al., 2006b). Despite possible ^{13}C enrichment during soil degradation (e.g. Chikaraishi and Naraoka, 2006), plant-derived lipid $\delta^{13}C$ values faithfully record the biosynthetic pathway of the producers and have thus been widely used to infer the relative contribution of C_3 and C_4 plants to soil organic matter (e.g. Rommerskirchen et al., 2006b; Diefendorf et al., 2011; Garcin et al., 2014).

The C_4 photosynthetic pathway occurs primarily within monocotyledonous plants and particularly among grasses (Poaceae) and sedges (Cyperaceae) (Ehleringer et al., 1997). Poaceae (graminoids) is a large family including more than 10,000 species that are particularly well represented in drier vegetation zones of tropical Africa (Tieszen et al., 1979). Pentacyclic triterpene methyl ethers (PTMEs) are found in variety of plants. But, because they typically occur in high abundance in C_4 graminoids (Poaceae; e.g. Ohmoto and Natori, 1969; Jacob et al., 2005), they have been used to infer grass contribution in geological records (Jacob et al., 2008; Oyo-Ita et al., 2010). Recently, they have been reported in substantial amount in savanna soil, making them attractive as a potential grass biomarker in C_4-dominated environments (Mendez-Millan et al., 2014).

Garcin et al. (2014) measured bulk and *n*-alkane $\delta^{13}C$ values of the common C_3 plants and C_4 graminoids of a climatic and vegetation gradient along a south–north transect in Cameroon. The transect was characterized by a progressive change in vegetation from C_3-dominated rainforest to C_4-dominated dry savanna and by a decrease in relative humidity (RH) from 80% to 45%. By comparing the $\delta^{13}C$ values of *n*-alkanes in plants and sediments against the relative abundance of C_3/C_4 plant cover in the region, Garcin et al. (2014) developed a new model to reconstruct C_3 vegetation cover in arid environments based on sedimentary *n*-alkane $\delta^{13}C$ records. Here, we have used bulk and *n*-alkane $\delta^{13}C$ values of the C_3 plants and C_4 graminoids from the former study to assess the photosynthetic origin of soil *n*-alkanes and PTMEs from the same study sites. By combining the $\delta^{13}C$ and δD values of these soil lipids, we aimed to differentiate the combined influences of climate and vegetation types (e.g. mostly C_3 trees and shrubs and C_4 graminoids) on leaf wax lipid δD values in the soil. The reliability of these lipids to record paleo-precipitation δD values and ecosystem evapotranspiration across the studied transect is discussed.

2. Study area

2.1. Climate

On the extreme south of the transect, the Debundscha (Debu), Ossa (Ossa) and Barombi (Baro) sites have a humid and hot climate with mean relative humidity (RH) ca. 85% (New et al., 2002) and mean annual temperature (MAT) ca. 26 °C. Precipitation (ca. 2500–12,000 mm/yr) occurs throughout the year, without a marked dry season (Table 1). Northwards, the length of the dry

Table 1
Climate and soil *n*-alkane and PTME distributions in the sampled lake catchments within different vegetation classes.

Latitude	Site code	Climate			Vegetation		Soil *n*-alkane and PTME distributions					
		RH[b] (%)	MAT[a] (°C)	MAP[a] (mm)	Zone[a]	f_{C3}[b]	Total *n*-alkanes (μg/g)	CPI (16–33)	CPI (25–33)	ACL (16–33)	Total PTMEs (μg/g)	% PTMEs
11.0547	Mora	45	27.2	540	DS	0.06 ± 0.06	270	2	6	24	50	16
10.5082	Rhum	46	22.7	970	DS	0.28 ± 0.25	480	3	8	25	150	24
7.2533	Mamg	57	26.3	1560	TZ	0.58 ± 0.06	340	3	7	26	60	15
7.1307	Tizo	63	21.8	1450	TZ	0.61 ± 0.05	370	4	8	25	100	22
6.6245	Tabe	63	21.7	1450	TZ	0.64 ± 0.04	610	11	18	28	10	2
5.0364	Asso	66	23	1740	TZ	0.69 ± 0.12	310	2	8	22	60	17
8.3909	Mane	77	16	2700	TZ (HA)	0.93[c] ± 0.12	1140	5	7	27	180	14
4.6544	Baro	81	24.9	2550	RF	0.95 ± 0.12	520	5	9	27	4	2
4.1034	Debu	82	25.7	11,700	RF	0.97 ± 0.12	1200	7	9	29	2	1
3.7686	Ossa	82	26.3	2900	RF	0.92 ± 0.19	360	19	20	29	1	1

CPI (16–33) = Σodd C*n*/Σeven C*n*; CPI (25–33) = $((C_{25}+C_{27}+C_{29}+C_{31}+C_{33}/C_{24}+C_{26}+C_{28}+C_{30}+C_{32}) + (C_{25}+C_{27}+C_{29}+C_{31}+C_{33}/C_{24}+C_{26}+C_{28}+C_{30}+C_{32}))/2$; ACL (16–33) = $(\Sigma Cn \times n)/\Sigma Cn$; %PTMEs = (ΣPTMEs)/ΣPTMEs + Σ*n*-alkanes) ∗ 100; RH = relative humidity; MAT = mean annual temperature; MAP = mean annual precipitation; RF = rainforest; TZ = transition zone; HA = high altitude site; DS = dry savanna; f_{C3} = predicted areal fraction of C_3 vegetation ± 1 standard deviation.

[a] From Garcin et al. (2012).
[b] From Garcin et al. (2014).
[c] Overestimated.

Table 2
Correlation matrix between the $\delta^{13}C$ and δD values of *n*-alkanes and PTMEs and between these lipid isotopic values and surface water δD values (δD_{sw}).

	δD_{sw}	δD_{C27}	$\delta^{13}C_{C27}$	δD_{C29}	$\delta^{13}C_{C29}$	δD_{C31}	$\delta^{13}C_{C31}$	δD_{C33}	$\delta^{13}C_{C33}$	δD_{saw}	$\delta^{13}C_{saw}$	δD_{mil}
δD_{sw}												
δD_{C27}	**0.85**											
$\delta^{13}C_{C27}$	**−0.85**	−0.62										
δD_{C29}	**0.83**	**0.99**	−0.56									
$\delta^{13}C_{C29}$	**−0.85**	**−0.77**	**0.91**	**−0.72**								
δD_{C31}	**0.80**	**0.88**	−0.59	**0.87**	**−0.82**							
$\delta^{13}C_{C31}$	**−0.77**	−0.51	**0.85**	−0.47	**0.90**	**−0.69**						
δD_{C33}	0.51	0.16	−0.50	0.14	−0.51	0.40	**−0.63**					
$\delta^{13}C_{C33}$	−0.51	−0.04	**0.73**	−0.01	0.55	−0.19	**0.77**	**−0.71**				
δD_{saw}	**0.86**	0.56	**−0.96**	0.51	**−0.84**	0.61	**−0.81**	**0.86**	**−0.92**			
$\delta^{13}C_{saw}$	−0.49	−0.10	**0.66**	−0.07	0.59	−0.42	**0.69**	**−0.92**	**0.96**	**−0.81**		
δD_{mil}	0.50	0.02	−0.40	0.12	0.08	−0.13	−0.42	−0.41	**−0.81**	**1.00**	**−1.00**	
$\delta^{13}C_{mil}$	0.41	0.45	−0.05	0.43	−0.33	0.64	−0.19	**0.82**	0.48	−1.00	**1.00**	−0.07

Numbers in bold are in a confidence interval of 95%; saw = sawamilletin, mil = miliacin.

season increases drastically, while mean annual precipitation (MAP), MAT and RH decrease. In the mountain ranges of western Cameroon, the Manengouba (Mane) site at ca. 2000 m above sea level (a.s.l.) has the most pronounced mountainous climate and the coolest MAT (ca. 18 °C) of the transect. MAP is high (2700 mm), with precipitation occurring throughout the year but maximizing from July to October. The Assom (Asso), Tabéré (Tabe) and Tizong (Tizo) sites are on the Adamawa Plateau, with an elevation of ca. 1000 m a.s.l. In the area, MAT is ca. 22 °C and the rainy season is limited to 7 months (April to November) with a MAP of ca. 1500 mm. The Mamguiewa (Mamg) site is on the southern edge of the North Region and has a rain pattern close to the sites of the Adamawa Plateau, with MAP ca. 1500 mm and MAT ca. 26 °C. Located in the northermost region, the Mora (Mora) and Rhumsiki (Rhum) sites are the driest sites on the transect. Rhum, at an altitude of 1000 m a.s.l. has mean RH ca. 45%, MAT ca. 23 °C and MAP ca. 700 mm/yr. Located on a lowland area (ca. 400 m a.s.l.), Mora has a close mean RH of ca. 45%, but higher MAT (ca. 27 °C) and lower MAP (ca. 500 mm/yr). At both of these drier sites, the dry season is longer (up to 7 months) and occurs from October to April.

2.2. Vegetation

The sites of the transect can be categorized, according to Mayaux et al. (1999) and White (1983), into three distinct main vegetation classes from south to north (Fig. 1). Close to the Atlantic coast, the Debu, Ossa and Baro sites are located in the vegetation of the rainforest, which is dominated by dense evergreen forest (Mayaux et al., 1999). The large canopy prevents the formation of shrubs and herbs that represent < 10% of the vegetation (Mayaux et al., 1999). In the transitional zone between the rainforest in the south and the dry savanna in the north, the vegetation of the Asso, Tabe, Tizo and Mamg sites is characterized by a tree savanna and woodland vegetation with up to 60% of shrubs and herbs (Mayaux et al., 1999). Deciduous trees lose their leaves briefly at different times, bringing a permanent green character to the canopy, while shrubs and herbs show a high degree of seasonality, with major growth during the rainy season (Mayaux et al., 1999). The high altitude site, Mane has a strongly disturbed Afromontane vegetation. Due to intensive pasture, the original forest, that covered ca. 30% of the lake catchment area, has been replaced mainly by grasses (Garcin et al., 2012). In the north, the Mora and Rhum sites are located in the dry savanna, dominated by C_4 grasses (Still and Powell, 2010). Shrubs are sparse and trees are located on the border of the water source (Mayaux et al., 1999). In this vegetation class, growth of both C_3 shrubs and C_4 grasses occurs mainly during the rainy season (Mayaux et al., 1999).

2.3. Isotope hydrology

The hydrogen isotope composition of plant xylem water, river water and groundwater, as well as precipitation from localized and sporadic rainfall events occurring in Cameroon during May, October and November 2009, were published by Garcin et al. (2012). As no mean annual precipitation δD values were available for the study area, surface water values (δD_{sw}) were estimated from these data. In summary, the average δD_{sw} values (−12.3 ± 3.7‰) for the Ossa, Debu and Baro sites on the Atlantic Coast were 15‰ heavier than the average δD_{sw} values (−26.8 ± 4.2‰) for the Mora and Rhum sites on the extreme north of the transect. The latitudinal intermediates, sites Asso, Tizo, Tabe and Mamg, showed average δD_{sw} values of −16 ± 1‰. The most D-depleted value of −38.9‰ was at the highest site, Mane, and reflected isotopically lighter precipitation due to the higher elevation.

3. Sampling and analytical procedure

3.1. Field sampling

Four to six topsoil (0–5 cm) samples from locations representative of vegetation in the lake catchment were collected using a hand-operated soil sampler (Eijkelkamp, Giesbeek, The Netherlands) in November 2009. Before analysis, the samples were sieved using a 400 μm mesh sieve to remove roots and other coarse material. The different soil samples were subsequently mixed and freeze-dried.

3.2. Lipid extraction and pre-treatment

To ensure a sufficient amount of PTMEs for hydrogen isotope analysis, ca. 20 g of each soil sample were prepared for extraction. As an internal standard, *n*-C_{37} (Sigma–Aldrich) was added to each freeze-dried sample prior to extraction with an automated solvent extractor (ASE-200, Dionex Corp., Sunnyvale, CA, USA). The system was operated with dichloromethane/methanol (DCM/MeOH) 9/1 at 120 °C, 2000 psi for 15 min in 3 cycles. The solvent was removed under a stream of N_2 using a rapidvap labconco system (Labconco Corporation, Kansas City, MO, USA). The extract was separated using column chromatography on pre-combusted and partially deactivated Al_2O_3 into three fractions: F1 eluted with hexane/DCM (9:1, v/v) and containing *n*-alkanes, F2 eluted with hexane/DCM (1:1, v/v) and containing the PTMEs, and F3 eluted with DCM/MeOH (1:1, v/v) and containing the alcohols. The *n*-alkanes in F1 and PTMEs in F2 were assigned and quantified using gas chromatography (GC) coupled via a splitter to a flame ionization

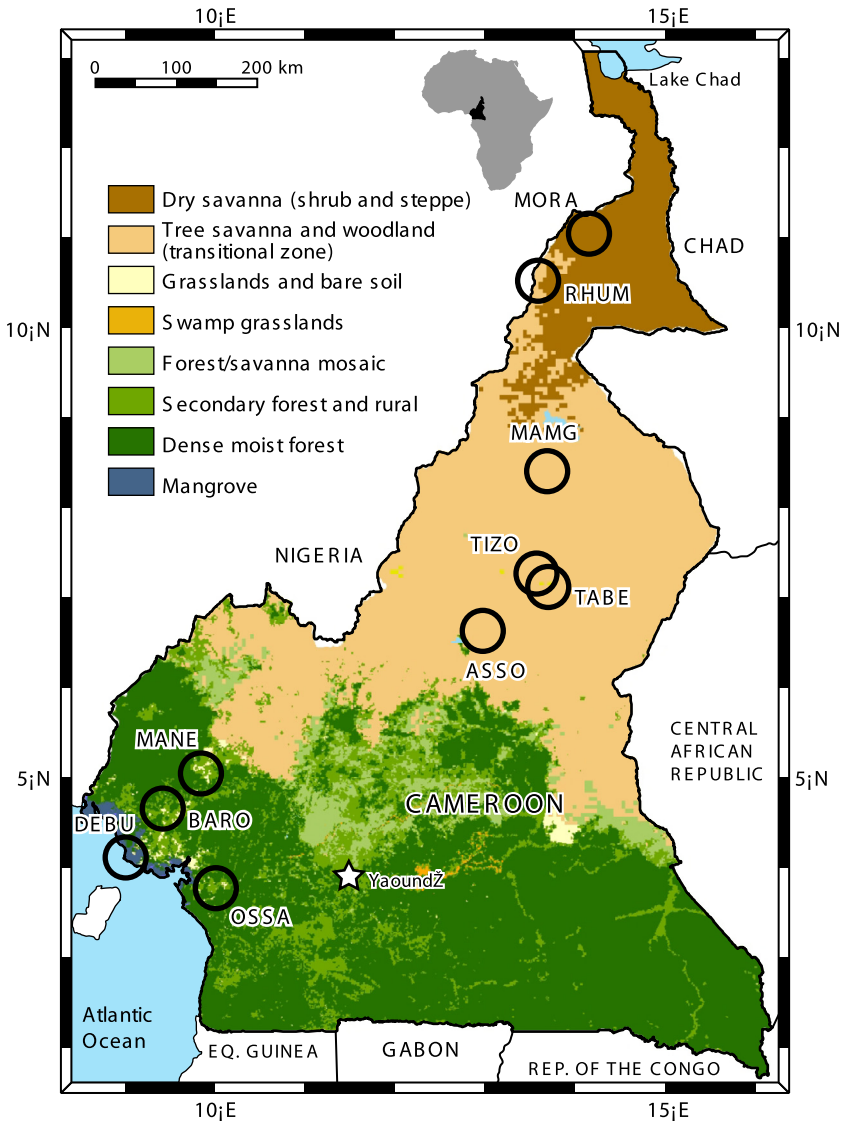

Fig. 1. Map showing the different vegetation classes for the Cameroon transect. Circles represent the locations of the study areas within the rainforest, transitional zone and dry savanna vegetation classes. The map was adapted from Mayaux et al. (2002) based on satellite imagery that provided a representation of the different ecosystem structures (plant types). Note that the highland vegetation of Mane is not differentiated.

detect or (FID; Agilent 7890A) and a quadrupole mass-selective detector (MSD; 5975C, Agilent Technologies, Palo Alto, USA) at the Biomarker Laboratory of the University of Potsdam. The GC instrument was equipped with a HP5-MS column (30 m, 0.25 mm, 0.25 μm film thickness). He was the carrier gas and the oven temperature program was: 70 °C (2 min) to 320 °C (held 21 min) at 11 °C/min. The PTV injector was operated splitless at an initial temperature of 70 °C. With injection, the injector was heated to 300 °C (held 2.5 min) at 720 °C/min. The PTMEs were assigned on the basis of published mass spectra (Jacob et al., 2005; Oyo-Ita et al., 2010). For quantification, FID peak areas were compared with those of the internal standard and an external *n*-alkane standard mixture at different concentrations.

3.3. Compound-specific carbon and hydrogen isotope analysis

Measurement of the carbon and hydrogen isotope composition of the *n*-alkanes and the PTMEs was performed using a GC-isotope ratio mass spectrometry (GC-IRMS) system (DeltaPlus XL, Finnigan MAT, Bremen, Germany) at the Max Planck Institute for Biogeochemistry, Jena. For hydrogen isotope analysis, the GC instrument (HP5890, Agilent Technologies, Palo Alto, USA) was equipped with a DB1-ms column (50 m, 0.32 mm i.d., 0.52 μm film thickness, Agilent). The injector at 280 °C was operated in splitless mode at a constant 1 ml/min. The oven temperature was maintained for 1 min at 60 °C, heated at 8 °C/min to 320 °C and held 30 min. For carbon isotope analysis, the gas chromatograph (HP5890, Agilent Technologies, Palo Alto, USA) was equipped with a DB1-ms column (30 m, 0.32 mm i.d., 0.52 μm film thickness, Agilent). The injector at 280 °C was operated in splitless mode at a constant flow of 1 ml/min. The oven temperature was maintained for 1 min at 70 °C, heated at 5 °C/min to 300 °C , held 15 min and then heated at 30 °C/min to 330 °C and held 3 min. Isotope values, expressed in the δ notation (‰), were calculated with ISODAT software vs. reference gas. The values were converted to the Vienna standard mean ocean water (VSMOW) scale using a mixture of *n*-alkanes (C_{17} to C_{33}) of known isotopic composition. The carbon and hydrogen isotope composition of the *n*-alkanes was determined off-line using a thermal conversion elemental analyzer (TC/EA: Thermo-Fisher, Bremen, Germany) interfaced to a DELTA V PLUS

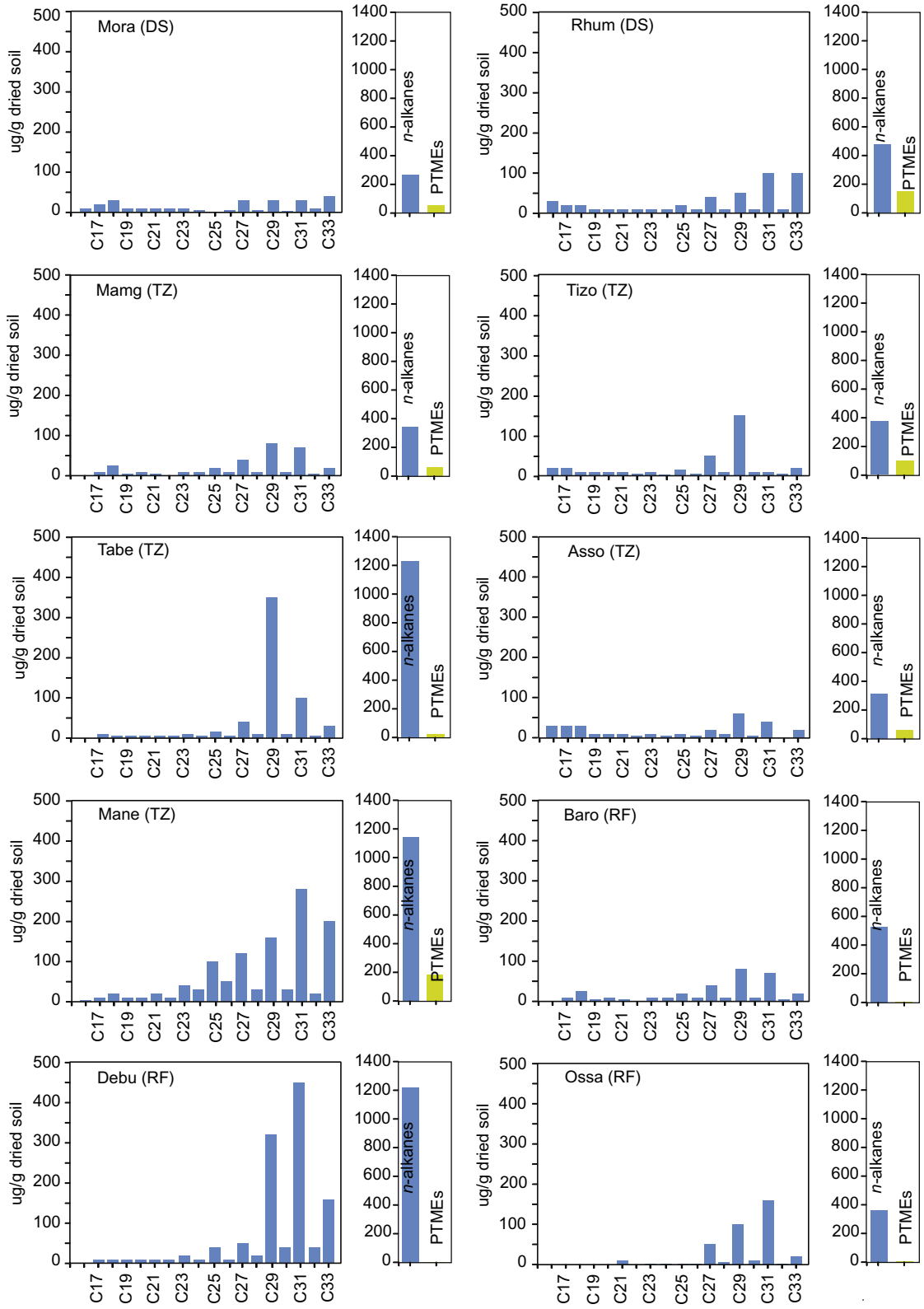

Fig. 2. Histograms of soil distributions and concentrations of total *n*-alkanes and total PTMEs. RF = rainforest; TZ = transition zone; DS = dry savanna.

IRMS system via a Conflo III combustion interface (Thermo-Fisher, Bremen, Germany). Instrument performance and the H_3^+ factor were determined on a daily basis using a tank of H_2 reference gas (Hilkert et al., 1999) and the mixture of *n*-alkanes (C_{17} to C_{33}) of known isotopic composition. The H_3^+ factor was < 11 and stable during analysis. We report isotopic fractionation between two substances, δD_a and δD_b, as enrichment factor ($\varepsilon_{a/b}$) defined as:

$$\varepsilon_{a/b} = \alpha_{a/b} - 1 = \frac{\delta D_a + 1}{\delta D_b + 1} - 1 \quad (1)$$

4. Results

4.1. Distribution and abundance of n-alkanes in soils

Soil *n*-alkanes ranged from C_{12} to C_{33} and displayed a strong predominance of long chain *n*-alkanes [average chain length (ACL from 22 to 29)] and high carbon preference index (CPI_{25-33} from 6 to 20; Table 1 and annex Table 1). The distributions in the vegetation classes of the rainforest and the transitional zone were dominated by *n*-C_{31} and *n*-C_{29}, respectively (Fig. 2). In the dry savanna, the distributions displayed an increase in the relative abundance of the longer chain *n*-alkanes that maximized at C_{33}. Concentration of individual *n*-alkanes ranged from < 1 to 450 μg/g dry mass (DM; annex Table 1). Total concentration of *n*-alkanes (from C_{16} to C_{33}) ranged from 260 to 1180 μg/g DM and showed an overall decrease toward the drier north of the transect (Table 1).

4.2. Distribution and abundance of PTMEs in soil

Various PTMEs, such as taraxer-14-en-3β-ol (sawamilletin), urs-12-en-3β-ol ME (α-amyrin ME), olean-18-en-3β-ol ME (miliacin), lup-20(29)-en-3β-ol (lupeol), fern-9(11)-en-3β-ol ME (arundoin) and arbor-9(11)-en-3β-ol ME (cylindrin) were observed in soil samples (annex Table 2). Typical distributions of the major PTMEs are shown in Fig. 3. Total concentration ranged from < 1 to 180 μg/g DM (Table 1) and the average tended to increase northward from < 1 μg/g DM in the rainforest to 150 μg/g DM in the dry savanna to > 180 μg/g DM at the high altitude site Mane (Table 1; Fig. 2). In samples from the rainforest, sawamilletin was the most abundant PTMEs at up to 2 μg/g DM, while in the dry savanna miliacin predominated at up to 140 μg/g DM. In samples from the transitional vegetation class, both sawamilletin (up to 50 μg/g) and miliacin (up to 120 μg/g) were dominant (annex Table 2). The concentrations of sawamilletin and miliacin (Table 1) relative to *n*-alkanes [PTMEs = (ΣPTMEs/ΣPTMEs + Σ*n*-alkanes) × 100 (%)] were significantly higher in the dry savanna (PTMEs ca. 20%) and the transitional zone (PTMEs ca. 14%) than the rainforest (PTMEs < 1%).

4.3. Carbon isotope composition of n-alkanes and PTMEs in soil

The $\delta^{13}C$ values of the long chain *n*-alkanes in common C_3 and C_4 plants of the study sites along the transect were presented by Garcin et al. (2014). In the soil samples, $\delta^{13}C$ values of *n*-C_{25}, *n*-C_{27}, *n*-C_{29}, *n*-C_{31} and *n*-C_{33} were in the range −40.9‰ to −18.1‰ (annex Table 3). In the dry savanna, the *n*-C_{25} to *n*-C_{33} values (mean −25.3 ± 3.2‰) were on average 9.2‰ more positive than those for the vegetation classes of the rainforest (mean −34.5 ± 3.5‰). In the transitional zone, the values of *n*-C_{25} to *n*-C_{33} were intermediate (mean −29.3 ± 3.7‰). At Mane, Asso, Tabe, Tizo and Mamg sites, the values for *n*-C_{33} (mean −23.1 ± 4.4‰) were up to 14‰ more positive than for the shorter chain homolog. In general, the $\delta^{13}C$ values for *n*-C_{27}, *n*-C_{29}, *n*-C_{31} and *n*-C_{33} correlated positively with each other, and negatively with δD_{sw} (Table 2).

Only sawamilletin and miliacin had sufficient concentration and purity for direct GC-IRMS analysis (annex Table 3). In the vegetation class of the rainforest, sawamilletin $\delta^{13}C$ values were −37.1‰ (Debu) and −38.1‰ (Baro). For the other vegetation classes, the values for sawamilletin and miliacin were similar, averaging −15.7‰ ± 0.8 and −15.5‰ ± 0.6, respectively. The $\delta^{13}C$ values of sawamilletin correlated positively with the those for *n*-C_{27}, *n*-C_{29}, *n*-C_{31} and *n*-C_{33} (Table 2).

4.4. Hydrogen isotope composition of n-alkanes and PTMEs in soil

The hydrogen isotope composition of *n*-C_{25}, *n*-C_{27}, *n*-C_{29}, *n*-C_{31} and *n*-C_{33} ranged from −142‰ to −172‰ (annex Table 4). In general, the δD values for *n*-C_{27}, *n*-C_{29} and *n*-C_{31} correlated with each other, while no correlation was observed between the δD values of *n*-C_{27-31} and *n*-C_{33} (Table 2). The hydrogen and carbon isotope composition of *n*-C_{29}, *n*-C_{31} and *n*-C_{33} were negatively correlated (Table 2).

In the rainforest class, the δD values of sawamilletin were −145‰ ± 1. At all other sites, sawamilletin (−172‰ ± 10) and miliacin (−169‰ ± 11) were both D depleted by 30‰ relative to sawamilletin from the rainforest (annex Table 4). Large differences in lipid δD values between *n*-alkanes and PTMEs were found in the vegetation class of the transitional zone, where PTME δD values were up to 21‰ more negative than *n*-alkane values. In this zone, the *n*-C_{33} δD values were intermediate between *n*-C_{27-31} and PTME δD values. In the vegetation classes of the rainforest and dry savanna, δD values of long chain *n*-alkanes and PTMEs were similar. The δD values of sawamilletin correlated positively with δD_{sw} values, but negatively with the $\delta^{13}C$ values of *n*-C_{27}, *n*-C_{29}, *n*-C_{31} and *n*-C_{33} (Table 2).

5. Discussion

5.1. Source of soil n-alkanes

The predominance of long chain *n*-alkanes with strong CPI (Table 1) in soil samples indicated their origin from higher plants (Eglinton and Hamilton, 1967). Common C_4 graminoids in Africa typically show a higher abundance of longer chain (> C_{31}) *n*-alkanes and $\delta^{13}C$ values up to 13‰ more positive than C_3 plants (e.g. Rommerskirchen et al., 2006a; Vogts et al., 2009; Bush and

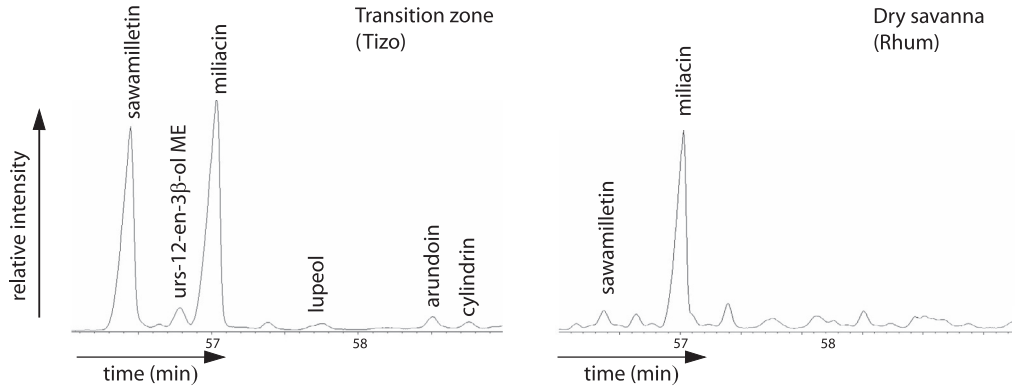

Fig. 3. Examples GC–MS traces for the major PTMEs in soil extracts.

McInerney, 2013). In geological records, a shift to longer chain and more ^{13}C-enriched *n*-alkanes is thus commonly attributed to vegetation changes from C_3 tree- to C_4 grass-dominated ecosystems (Rommerskirchen et al., 2006b). However, it is well known that leaf bulk $\delta^{13}C$ values of C_3 plants may also be affected by the physiological response of the plant to aridity (Farquhar et al., 1989), with $\delta^{13}C$ values above −25‰ in environments with MAP < 500 mm/yr and $\delta^{13}C$ values around −30‰ in environments with MAP > 1000 mm/yr (Stewart et al., 1995; Kohn, 2010; Diefendorf et al., 2011). At the sites along the transect, Garcin et al. (2014) showed that lacustrine sedimentary *n*-C_{29} and *n*-C_{31} were derived mainly from C_3 plants (mostly trees and shrubs) and their ^{13}C enrichment along the latitudinal gradient likely reflected a physiological response of C_3 plants to aridity rather than an increasing contribution of C_4 plants to the sediments. In line with this interpretation, we argue that the ^{13}C-enrichment of *n*-C_{29} and *n*-C_{31} in soils from the study sites, recorded mainly the physiological response of C_3 plants to aridity, as the slope of the correlation of the *n*-alkane $\delta^{13}C$ values in soil vs. RH was identical to the slope of the correlation of the *n*-alkane $\delta^{13}C$ values in the major C_3 plants of the area vs. RH (Fig. 4A and B). In the transitional zone, particularly at the Mane and Asso sites, soil *n*-C_{33} $\delta^{13}C$ values showed a different trend, exhibiting more positive $\delta^{13}C$ values (Fig. 4C) likely due to a greater contribution of C_4 graminoid-derived *n*-C_{33}. The results showed that, along the transect, soil *n*-C_{29} and *n*-C_{31} probably better constrained the isotope signal of C_3 plants than C_4 graminoids, whereas soil *n*-C_{33} δD values that integrated a higher proportion of C_4 graminoids may give a mixed signal of the different plant types.

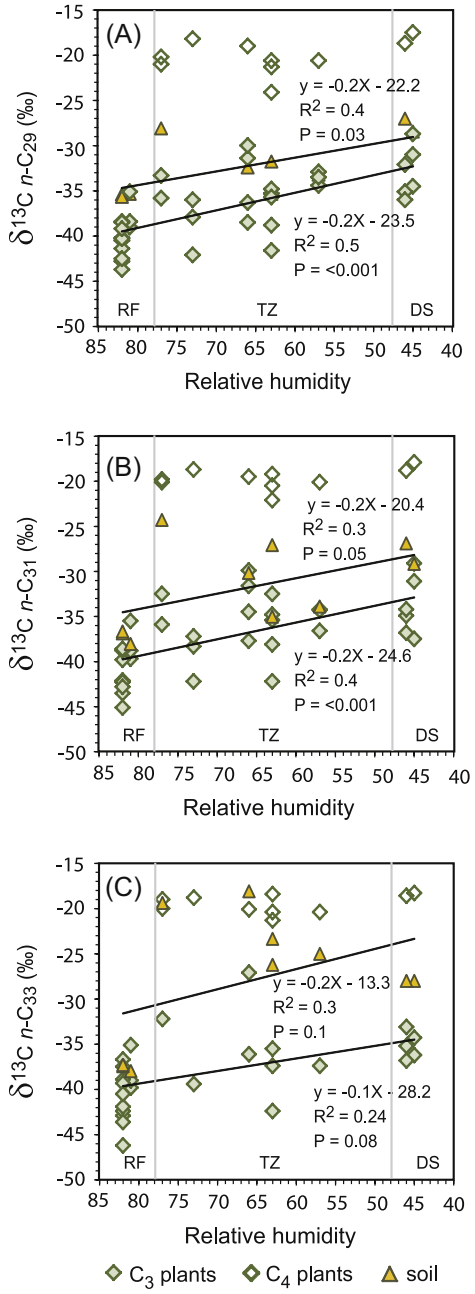

Fig. 4. Carbon isotope composition of soil *n*-C_{29}, *n*-C_{31} and *n*-C_{33} vs. relative humidity. For comparison, carbon isotope composition of the corresponding *n*-alkanes in the major C_3 plants and C_4 plants are represented (Garcin et al., 2014). RF = rainforest; TZ = transition zone; DS = dry savanna. Error bars are smaller than data points; see annex Table 3 and Garcin et al. (2014) for details.

5.2. Source of soil PTMEs

In soil samples from the transitional zone and dry savanna, the $\delta^{13}C$ values of miliacin and sawamilletin were ca. 4‰ more negative than those of leaf bulk of common C_4 plants (Fig. 5), supporting the C_4 biosynthetic origin of the soil PTMEs (e.g. Chikaraishi et al., 2004; Diefendorf et al., 2011). In the rainforest class, sawamilletins ^{13}C depleted by ca. 3‰ relative to leaf bulk of common C_3 plants, supported a biosynthetic origin from the C_3 pathway for this compound (Fig. 5).

Common and important C_4 producers of miliacin are the domesticated *Pennisetum sp.* and *Panicum miliaceum* (Jacob et al., 2008; Bossard et al., 2011). The occurrence of these species associated, with the high concentration of miliacin in the northern dryer sites of the transect (up to 150 μg/g DM: Table 1), support the statement that miliacin may possibly be used to track past millet agriculture dynamics (Bossard et al., 2013). Some Eragrosteae as *Eragrostis ferrigunea* have been additionally described as important C_4 producers of miliacin (Jacob et al., 2005). The occurrence of different species of this genus in sites of the transitional zone and dry savanna (Garcin et al., 2012) suggested that Eragrosteae may be an additional important source of miliacin in geological records. Common C_4 graminoid producers of sawamilletin are some Panicoideae such as *Saccharum robustum* (sugar-cane: Smith and Martin-Smith, 1978) and *Miscanthus sacchariflorus* or *Echinochloa crusgalli* (Jacob et al., 2005), which are common in wet (MAP > 1000 mm/yr)

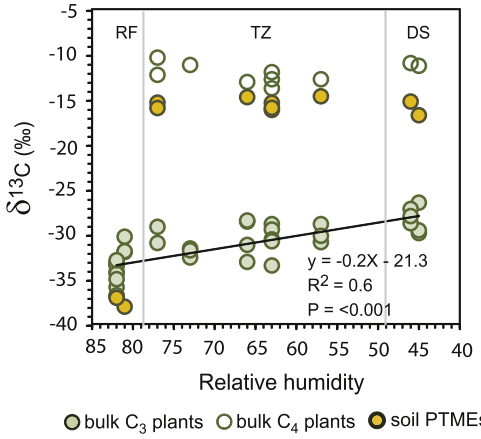

Fig. 5. Carbon isotope composition of soil PTMEs vs. relative humidity. For comparison, carbon isotope composition of leaf bulk of the major C_3 plants and C_4 plants are represented (Garcin et al., 2014). RF = rainforest; TZ = transition zone; DS = dry savanna. Error bars are smaller than data points; see annex Table 3 and Garcin et al. (2014) for details.

environments. C_3 graminoids are commonly referred to as perennial "cool-seasonal" grass such as some Poeae such as *Festuca* spp., *Poa pratensis or* C_3 *panicum* species which, in the tropical forest, are particularly represented in shaded habitat and may represent ca. 40% of the total grasses (Klink and Joly, 1989). However, as sawamilletin has not been reported in these grasses, an origin of C_3-derived sawamilletin at the sites of the rainforest from C_3 trees such as *Diospyros* spp. (Ebenaceae) and *Bosisstoa* spp. (Rutaceae) is more likely (Jacob et al., 2005).

In the transect, the change from the rainforest to the transition zone was characterized by a ca. 15% drop in the C_3 vegetation cover (Table 1). This vegetation change was recorded in soil by a sharp increase of the PTME concentration and PTME/*n*-alkane ratios (Table 1 and Fig. 2). These observations support previous statement that PTMEs are produced mainly by C_4 graminoids (Jacob et al., 2005) and suggest that in tropical and sub-tropical soil records increasing concentration of PTMEs relative to *n*-alkanes may be used to infer vegetation change from rainforest to transition zone.

5.3. Soil n-alkane and PTME δD values vs. surface water δD values

Similarly biosynthesized compounds generally display a positive correlation in δD to each other as well as their $\delta^{13}C$ values (Chikaraishi et al., 2004). Along the transect, the correlation of δD and $\delta^{13}C$ values for *n*-C_{27}, *n*-C_{29} and *n*-C_{31} were in line with a common C_3 plant origin. In contrast, the absence of the above correlation between these *n*-alkanes and *n*-C_{33} suggests a different biosynthetic source for *n*-C_{33} in the soils. Based on *n*-C_{33} $\delta^{13}C$ values, a higher contribution of C_4 graminoids to soil *n*-C_{33} seems plausible (Table 2). The significant correlation between δD_{sw} and δD values for mainly C_3 plant-derived *n*-alkanes (Fig. 6) demonstrated that leaf wax lipid δD values are an effective proxy for reconstructing average precipitation δD values, despite large vegetation changes (e.g. Sachse et al., 2006; Liu and Yang, 2008; Garcin et al., 2012). As *n*-C_{33} included a higher proportion of C_4 graminoid than *n*-C_{27-31} alkanes, we suggest that different contributions from C_3 and C_4 plants resulted in the insignificance of the correlation between *n*-C_{33} and surface water δD values (Fig. 6). However, this may also be associated with the fact that δD values of *n*-C_{33} could not be measured at the Mane site with the lightest δD_{sw} values. The δD values of PTMEs from C_3 and C_4 pathways correlated significantly with δD_{sw} (Fig. 7). However, the correlation becomes at the limit of the statistical significance ($p = 0.08$) when only the δD values of C_4 graminoid-derived PTMEs are used. In arid and semi-arid environments, it has been shown that C_3 plant-derived lipids record mean annual precipitation δD values, as they use subsurface water which is not or slightly affected by soil water evaporative D enrichment (Feakins and Sessions, 2010; Kahmen et al., 2013b). In contrast, lipid δD values in graminoids that use surface soil water would potentially be more affected by soil water evaporative D enrichment. This may have contributed to lower significance in the correlation between δD values of C_4 graminoids derived PTMEs and surface water δD values along the transect.

5.4. Aridity effect on lipid δD values of C_3 plants and C_4 graminoids

Since leaf wax lipid δD values in both C_3 and C_4 plants are decisively influenced by leaf water evaporative D enrichment (Kahmen et al., 2013a,b), the apparent fractionation between lipids and source water (ε_{app}) should theoretically decrease with aridity. However, along the latitudinal gradient covering a RH range from 80% to 45%, the ε_{app} of inferred C_3 plant-derived *n*-alkanes remained relatively constant at −140‰ (Fig. 8). Plant functional type has an important control on leaf wax lipid δD values. Different lipid δD values may reflect different growth mechanisms,

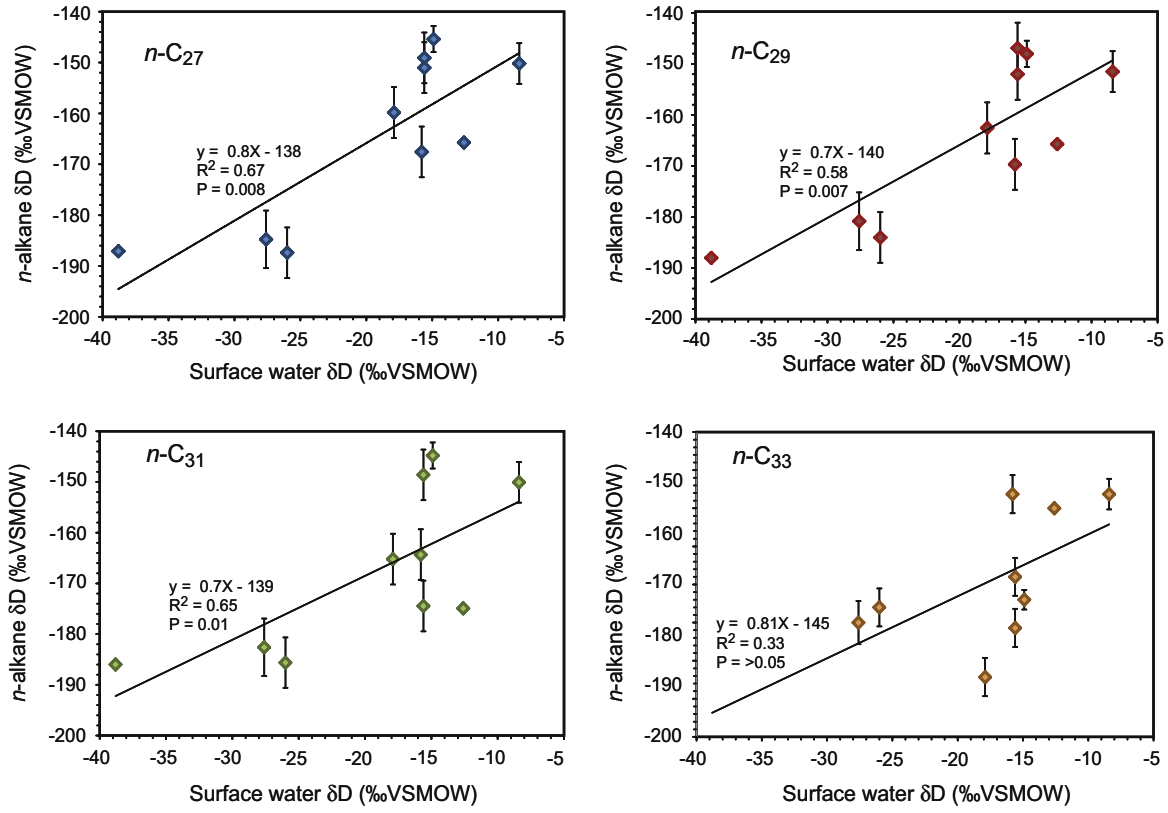

Fig. 6. Hydrogen isotope composition of soil *n*-C_{27}, *n*-C_{29}, *n*-C_{31} and *n*-C_{33} vs. surface water δD values.

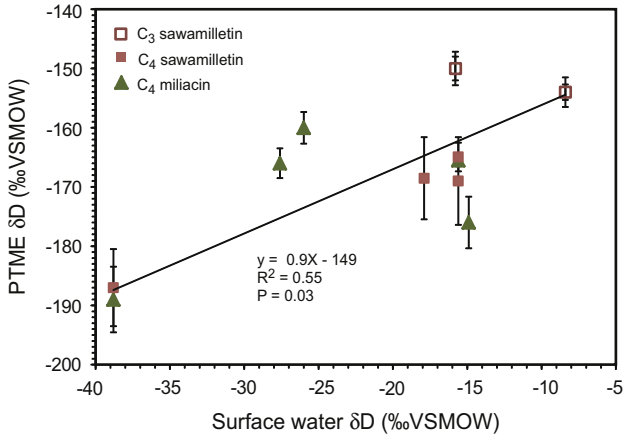

Fig. 7. Hydrogen isotope composition of soil PTME vs. surface water δD values.

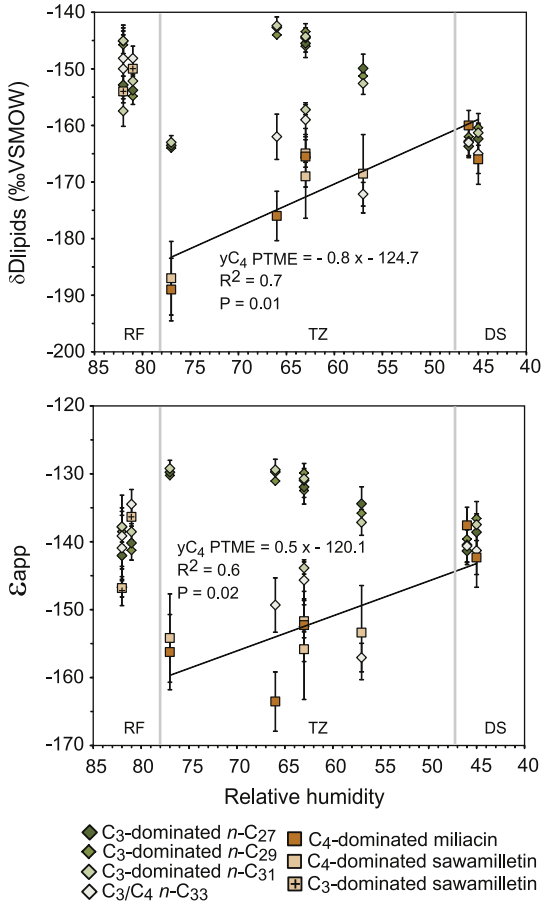

Fig. 8. Hydrogen isotope composition (top) and fractionation factor (ε_{app}) (bottom) of soil *n*-C_{27}, *n*-C_{29}, *n*-C_{31} and *n*-C_{33} and soil PTMEs vs. relative humidity. The ε_{app} was calculated against surface water. The biosynthetic pathway has been assigned according to the lipid $\delta^{13}C$ values. The regression lines were calculated using the values of both PTMEs, e.g. sawamilletin and miliacin, derived from the C_4 biosynthetic pathway. RF = rainforest; TZ = transition zone; DS = dry savanna.

magnitude of leaf water D enrichment and/or (seasonal) water sources related to differences in seasonal growth or root pattern (Sachse et al., 2010, 2012; Kahmen et al., 2013a). The influence of evapotranspiration on the isotopic enrichment of plant biosynthetic water and consequently on leaf wax lipid δD values driven by aridity is thus expected to become apparent when the other drivers co-vary in one direction. Conversely, counteracting drivers may cancel the effects of aridity recorded in leaf wax lipid δD values. Here, C_3 vegetation change is particularly important between the transitional zone and the dry savanna, where shrubs replaced trees (Mayaux et al., 1999). In such environments, characterized by long periods of seasonal drought and low annual precipitation amount, the seasonal growth pattern of plants is related mainly to a plant's ability to maintain a constant water supply throughout the year (e.g. Dawson and Pate, 1995; Dawson et al., 2002; Mayaux et al., 2004). Shrubs with a more shallow rooting system than trees cannot meet their water demand throughout the year and thus develop a growth cycle related to seasonality of rainfall, entering in to a dormancy period during the dry season (Mayaux et al., 2004). In contrast, C_3 trees with a deeper rooting pattern can exploit subsurface water throughout the year (groundwater) and develop an annual growth pattern (Schulze, 1986; Dawson and Pate, 1995; Oliveira et al., 2005). Recent research has shown that the majority of leaf wax development probably takes place during a relatively short period of leaf development (Kahmen et al., 2011; Tipple et al., 2013). Therefore, as precipitation δD values during the rainy season in the tropics are typically more negative (by ca. 20‰) than the mean annual precipitation δD values (Rozanski et al., 1993; Rozanski and Araguas, 1995), leaf wax lipids from C_3 plants with an optimum growth during the rainy season (e.g. shrubs) will likely be more D depleted than lipids from plants with an annual growth pattern (e.g. trees: Sachse et al., 2009; Polissar and Freeman, 2010). In addition, leaf and surface soil water isotopic enrichment is expected to be minimal during the wet season, owing to the high relative humidity during these months. Therefore, it can be hypothesized that, especially in the north of the transect, C_3 plant-derived leaf wax lipids are produced mainly during the wet season, thereby resulting in the constancy of long chain *n*-alkane ε_{app} values along the transect.

On the other hand, the C_4 graminoid vegetation type in the transitional zone and dry savanna remains similar (Ehleringer et al., 1997; Still et al., 2003) and with a shallower rooting system than trees and brushes, graminoids access more evaporatively D enriched surface soil water (Schulze et al., 1996). This may partially explain why C_4 graminoids PTME δD values were more affected by aridity and the associated soil and leaf water D enrichment than C_3 plant *n*-alkanes, and showed a 20‰ increase in ε_{app} toward the drier North (Fig. 8). Furthermore, assuming a constant temperature of 20 °C and equilibrium conditions between atmospheric water vapor and plant source water, current leaf water isotope models (Kahmen et al., 2013a) would suggest an increase in leaf water D enrichment of ca. 30‰ during a change in RH from 80% to 45%. Therefore, the observation of a 20‰ difference in ε_{app} is in line with the observation that C_4 grasses only partially used (68% was estimated for C_4 grasses) evaporatively D enriched leaf water for lipid biosynthesis (Sachse et al., 2009; Kahmen et al., 2013a). In summary, our results indicate that δD values of C_4 graminoid-derived PTMEs may be a more reliable paleo-ecohydrological proxy for ecosystem evapotranspiration in tropical and sub-tropical Africa than C_3 plant-derived *n*-alkanes, the latter being a better proxy for surface water (or average precipitation) δD values.

Our PTME δD values were measured in soil of the lake catchments and thus do not provide information on a possible correlation between sedimentary PTME δD values and relative humidity. However, the close patterns between sedimentary, soil and plant *n*-alkane $\delta^{13}C$ values (Garcin et al., 2014) in the study sites suggested that soil erosion is the major source of terrestrial biomarkers in the lake sediments and thus that sedimentary PTMEs should have similar isotopic patterns to our soil PTMEs.

6. Paleoenvironmental implications

As C_3 and C_4 plants synthetize *n*-alkanes with different hydrogen isotope composition (Sachse et al., 2012; Kahmen et al., 2013a), in geological records *n*-alkane δD values are commonly used in combination with *n*-alkane $\delta^{13}C$ values to evaluate changes in the relative contribution of C_3 plant and C_4 plant-derived *n*-alkanes, and in turn to better separate climatic and physiological controls on their integrated hydrogen isotope compositions. We have shown here that different morphology, seasonal growth and/or different timing of leaf wax synthesis in C_3 plants may cancel the effect of aridity on C_3 plant-derived *n*-alkanes in soil. This implies that, even when assessing the C_3 photosynthetic origin of *n*-alkanes based on their $\delta^{13}C$ values, changes in the C_3 plant community may bias the aridity signal on C_3 plant-derived *n*-alkane δD values in geological records. Therefore, only a combination of species identification based on pollen or biomarker records associated with both *n*-alkane δD and $\delta^{13}C$ analyses ought to provide maximum interpretive value to accurately separate climatic and physiological controls on *n*-alkane δD values in geological records.

Our study suggests that biomarkers, such as PTMEs, that have a dominant plant source in a given environmental context ought to give a more unequivocal hydrogen isotopic signature than *n*-alkanes. Soil PTME δD values derived from C_4 graminoids better recorded aridity than soil leaf wax *n*-alkanes inferred to be derived mainly from C_3 plants. This suggests that these lipids may be an accurate proxy for paleoenvironmental reconstruction in tropical dry Africa, since their δD values are potentially not significantly affected by changes in plant community and growth form. However, in rainforest environments, the δD values of C_3 plant-derived sawamilletin were by 20‰ more positive than C_4 plant-derived sawamilletin δD values in the drier vegetation zones. Such a difference implies that a different contribution from C_3 plant- and C_4 plant-derived sawamilletin may potentially bias the effect of aridity on its integrated δD values in geological records. Although miliacin can be produced by both C_4 and C_3 plants, it was dominantly produced by C_4 graminoids in soil along the transect. This suggests that miliacin may potentially be a more reliable proxy than sawamilletin for C_4 graminoids and, thus, that its δD values may better record ecosystem aridity in tropical Africa.

We found a substantial concentration of sawamilletin and miliacin (up to 140 μg/g DM) relative to long chain *n*-alkanes (up to 350 μg/g DM) in soil of the transition zone and dry savanna (annex Tables 1 and 2). Similarly, relative high concentrations of these PTMEs or diagenetically derived product iso-sawamilletin were recently measured in savanna soil (Mendez-Millan et al., 2014) or lake sediment (Jacob et al., 2005), suggesting that PTMEs may potentially become a significant C_4 graminoid proxy for drier vegetation zones of Africa. In contrast, in the rainforest PTMEs derived from graminoids were not detected (or were in low concentration), indicating that in cooler and wetter environments, alternative graminoid biomarkers, potentially such as ferulic acid methyl ester which was detected in *Eriophorum vaginatum* (Schellekens et al., 2013) may be more suitable.

7. Conclusions

By comparing *n*-alkane $\delta^{13}C$ values of the major C_3 and C_4 plants with the $\delta^{13}C$ values of soil long chain *n*-alkanes at the sites from a latitudinal gradient in C_3/C_4 vegetation and aridity in Cameroon, we inferred that soil *n*-C_{29} and *n*-C_{31} were derived mainly from C_3 plants (e.g. trees and shrubs), while the *n*-C_{33} included a greater contribution from C_4 graminoids. In the vegetation classes of the transitional zone and the dry savanna, $\delta^{13}C$ values of PTMEs (mean −15.6‰), including both sawamilletin and miliacin, supported a C_4 graminoid origin, whereas in the rainforest class, up to 24‰ ^{13}C-depleted sawamilletin suggested a C_3 plant origin. The significant correlations of the δD values of *n*-C_{29} and *n*-C_{31}, and PTMEs with surface water δD values (δD_{sw}) further demonstrated that leaf wax lipid δD values are an effective proxy for reconstructing mean annual precipitation δD values. Along the latitudinal gradient, covering a relative humidity range from 80% to 45%, the apparent fractionation (ε_{app}) between the *n*-alkanes, inferred to be derived mainly from C_3 plants, and surface water remained relatively constant, whereas ε_{app} for C_4 graminoid-derived PTMEs increased by 20‰ with decreasing relative humidity. We hypothesize that vegetation change associated with different plant water sources and/or different seasonal growth periods of leaf wax synthesis resulted in a relatively constant fractionation factor in C_3 plants, whereas for C_4 graminoids these former factors were constant enough to record the effect evaporative D enrichment driven by aridity on PTME δD values.

Acknowledgments

These research was supported by the MPI-BGC Jena (to V.F.S. and G.G.) and by the German Science Foundation (DFG) to Y.G. (GA-1629/1-1&2) and through the DFG Emmy-Noether Programme to D.S. (SA-1889/1-1) and the DFG Leibniz Center for Surface Process and Climate Studies at Potsdam University (to Y.G. and D.S.). We are grateful to the Ministry of Scientific Research and Innovation of Cameroon (Research Permit 54/MINRESI/B00/C00/C10/C13) and the "Institut de Recherche pour le Développement (IRD)" for administrative and logistical support. We are also grateful to Y. Chikaraishi and an anonymous reviewer for critical comments that greatly improved the quality of the manuscript.

Appendix A. Supplementary material

Supplementary data associated with this article can be found, in the online version, at http://dx.doi.org/10.1016/j.orggeochem.2014.09.007.

Associate Editor—**S. Schouten**

References

Bi, X., Sheng, G., Liu, X., Li, C., Fu, J., 2005. Molecular and carbon and hydrogen isotopic composition of *n*-alkanes in plant leaf waxes. Organic Geochemistry 36, 1405–1417.

Bossard, N., Jacob, J., Le Milbeau, C., Lallier-Verges, E., Terwilliger, V.J., Boscardin, R., 2011. Variation in delta D values of a single, species-specific molecular biomarker: a study of miliacin throughout a field of broomcorn millet (*Panicum miliaceum L.*). Rapid Communications in Mass Spectrometry 25, 2732–2740.

Bossard, N., Jacob, J., Le Milbeau, C., Sauze, J., Terwilliger, V., Poissonnier, B., Vergès, E., 2013. Distribution of miliacin (olean-18-en-3β-ol methyl ether) and related compounds in broomcorn millet (*Panicum miliaceum*) and other reputed sources: implications for the use of sedimentary miliacin as a tracer of millet. Organic Geochemistry 63, 48–55.

Bush, R.T., McInerney, F.A., 2013. Leaf wax *n*-alkane distributions in and across modern plants: implications for paleoecology and chemotaxonomy. Geochimica et Cosmochimica Acta 117, 161–179.

Chikaraishi, Y., Naraoka, H., 2006. Carbon and hydrogen isotope variation of plant biomarkers in a plant–soil system. Chemical Geology 231, 190–202.

Chikaraishi, Y., Naraoka, H., 2007. $\delta^{13}C$ and δD relationships among three *n*-alkyl compound classes (*n*-alkanoic acid, *n*-alkane and *n*-alkanol) of terrestrial higher plants. Organic Geochemistry 38, 198–215.

Chikaraishi, Y., Naraoka, H., Poulson, S.R., 2004. Carbon and hydrogen isotopic fractionation during lipid biosynthesis in a higher plant (*Cryptomeria japonica*). Phytochemistry 65, 323–330.

Dawson, T.E., Pate, J.S., 1995. Seasonal water uptake and movement in root systems of Australian phreatophytic plants of dimorphic root morphology: a stable isotope investigation. Oecologia 107, 13–20.

Dawson, T.E., Mambelli, S., Plamboeck, A.H., Templer, P.H., Tu, K.P., 2002. Stable isotopes in plant ecology. Annual Review of Ecology and Systematics 33, 507–559.

Diefendorf, A.F., Freeman, K.H., Wing, S.L., Graham, H.V., 2011. Production of *n*-alkyl lipids in living plants and implications for the geologic past. Geochimica et Cosmochimica Acta 75, 7472–7485.

Eglinton, G., Hamilton, R.J., 1967. Leaf epicuticular waxes. Science 156, 1322–1335.
Ehleringer, J.R., Cerling, T.E., Helliker, B.R., 1997. C_4 photosynthesis, atmospheric CO_2, and climate. Oecologia 112, 285–299.
Farquhar, G.D., Ehleringer, J.R., Hubick, K.T., 1989. Carbon isotope discrimination and photosynthesis. Annual Review of Plant Physiology and Plant Molecular Biology 40, 503–537.
Feakins, S.J., Sessions, A.L., 2010. Controls on the D/H ratios of plant leaf waxes in an arid ecosystem. Geochimica et Cosmochimica Acta 74, 2128–2141.
Garcin, Y., Schwab, V.F., Gleixner, G., Kahmen, A., Todou, G., Séné, O., Onana, J.-M., Achoundong, G., Sachse, D., 2012. Hydrogen isotope ratios of lacustrine sedimentary *n*-alkanes as proxies of tropical African hydrology: insights from a calibration transect across Cameroon. Geochimica et Cosmochimica Acta 79, 106–126.
Garcin, Y., Schefuß, E., Schwab, V.F., Garreta, V., Gleixner, G., Vincens, A., Todou, G., Séné, O., Onana, J.-M., Achoundong, G., Sachse, D., 2014. Reconstructing C_3 versus C_4 vegetation cover using *n*-alkane carbon isotopes – a surface sediment test from Cameroon, Western Central Africa. Geochimica Cosmochimica Acta 142, 482–500.
Guenther, F., Aichner, B., Siegwolf, R., Xu, B., Yao, T., Gleixner, G., 2013. A synthesis of hydrogen isotope variability and its hydrological significance at the Qinghai-Tibetan Plateau. Quaternary International 313–314, 3–16.
Handley, L., O'Halloran, A., Pearson, P.N., Hawkins, E., Nicholas, C.J., Schouten, S., McMillan, I.K., Pancost, R.D., 2012. Changes in the hydrological cycle in tropical East Africa during the Paleocene–Eocene Thermal Maximum. Palaeogeography, Palaeoclimatology, Palaeoecology 329–330, 10–21.
Hilkert, A.W., Douthitt, C.B., Schluter, H.J., Brand, W.A., 1999. Isotope ratio monitoring gas chromatography mass spectrometry of D/H by high temperature conversion isotoperatio mass spectrometry. Rapid Communication in Mass Spectrometry 13, 1226–1230.
Hou, J.Z., D'Andrea, W.J., Huang, Y., 2008. Can sedimentary leaf waxes record D/H ratios of continental precipitation? Field, model, and experimental assessments. Geochimica et Cosmochimica Acta 72, 3503–3517.
Jacob, J., Disnar, J., Boussafir, M., Spadanoalbuquerque, A., Sifeddine, A., Turcq, B., 2005. Pentacyclic triterpene methyl ethers in recent lacustrine sediments (Lagoa do Caço, Brazil). Organic Geochemistry 36, 449–461.
Jacob, J., Disnar, J.-R., Bardoux, G., 2008. Carbon isotope evidence for sedimentary miliacin as a tracer of *Panicum miliaceum* (broomcorn millet) in the sediments of Lake le Bourget (French Alps). Organic Geochemistry 39, 1077–1080.
Kahmen, A., Dawson, T.E., Vieth, A., Sachse, D., 2011. Leaf wax *n*-alkane δD values are determined early in the ontogeny of *Populus trichocarpa* leaves when grown under controlled environmental conditions. Plant Cell Environment 34, 1639–1651.
Kahmen, A., Schefuß, E., Sachse, D., 2013a. Leaf water deuterium enrichment shapes leaf wax *n*-alkane δD values of angiosperm plants I: experimental evidence and mechanistic insights. Geochimica et Cosmochimica Acta 111, 39–49.
Kahmen, A., Hoffmann, B., Schefuß, E., Arndt, S.K., Cernusak, L.A., West, J.B., Sachse, D., 2013b. Leaf water deuterium enrichment shapes leaf wax *n*-alkane δD values of angiosperm plants II: observational evidence and global implications. Geochimica et Cosmochimica Acta 111, 50–63.
Klink, C.A., Joly, C.A., 1989. Identification and distribution of C_3 and C_4 grasses in open and shaded habitats in Sao Paulo State, Brazil. Biotropica 21, 30–34.
Kohn, M.J., 2010. Carbon isotope compositions of terrestrial C_3 plants as indicators of (paleo)ecology and (paleo)climate. Proceedings of the National Academy of Sciences of the United States of America 107, 19691–19695.
Krull, E., Sachse, D., Mügler, I., Thiele, A., Gleixner, G., 2006. Compound-specific $\delta^{13}C$ and $\delta^{2}H$ analyses of plant and soil organic matter: a preliminary assessment of the effects of vegetation change on ecosystem hydrology. Soil Biology and Biochemistry 38, 3211–3221.
Liu, W., Yang, H., 2008. Multiple controls for the variability of hydrogen isotopic compositions in higher plant *n*-alkanes from modern ecosystems. Global Change Biology 14, 2166–2177.
Mayaux, P., Richards, T., Janodet, E., 1999. A vegetation map of Central Africa derived from satellite imagery. Journal of Biogeography 26, 353–366.
Mayaux, P., De Grandi, G.F., Rauste, Y., Simard, M., Saatchi, S., 2002. Large scale vegetation maps derived from the combined L-band GRFM and C-band CAMP wide area radar mosaics of Central Africa. International Journal of Remote Sensing 23, 1261–1282.
Mayaux, P., Bartholomé, E., Fritz, S., Belward, A., 2004. A new land-cover map of Africa for the year 2000. Journal of Biogeography 31, 861–877.
Mendez-Millan, M., Nguyen Tu, T.T., Balesdent, J., Derenne, S., Derrien, D., Egasse, C., Thongo M'Bou, A., Zeller, B., Hatté, C., 2014. Compound-specific ^{13}C and ^{14}C measurements improve the understanding of soil organic matter dynamics. Biogeochemistry 118, 205–223.
Mügler, I., Gleixner, G., Günther, F., Mausbacher, R., Daut, G., Schutt, B., Berking, J., Schwalb, A., Schwark, L., Xu, B., Yao, T., Zhu, L., Yi, C., 2010. A multi-proxy approach to reconstruct hydrological changes and Holocene climate development of Nam Co, Central Tibet. Journal of Paleolimnology 43, 625–648.
New, M., Lister, D., Hulme, M., Makin, I., 2002. A high-resolution data set of surface climate over global land areas. Climate Research 21, 1–25.
Ohmoto, T., Natori, S., 1969. Triterpene methyl ethers from Gramineae plants: lupeol methyl ether, 12-oxoarundoin, and arborinol methyl ether. Journal of the Chemical Society D: Chemical Communications, 601a.
Oliveira, R., Dawson, T., Burgess, S.O., Nepstad, D., 2005. Hydraulic redistribution in three Amazonian trees. Oecologia 145, 354–363.
Oyo-Ita, O.E., Ekpo, B.O., Oros, D.R., Simoneit, B.R.T., 2010. Occurrence and sources of triterpenoid methyl ethers and acetates in sediments of the cross-river system, Southeast Nigeria. International Journal of Analytical Chemistry 2010, 1–8.
Polissar, P.J., Freeman, K.H., 2010. Effects of aridity and vegetation on plant-wax δD in modern lake sediments. Geochimica et Cosmochimica Acta 74, 5785–5797.
Rommerskirchen, F., Plader, A., Eglinton, G., Chikaraishi, Y., Rullkötter, J., 2006a. Chemotaxonomic significance of distribution and stable carbon isotopic composition of long-chain alkanes and alkan-1-ols in C_4 grass waxes. Organic Geochemistry 37, 1303–1332.
Rommerskirchen, F., Eglinton, G., Dupont, L., Rullkötter, J., 2006b. Glacial/interglacial changes in southern Africa: compound-specific $\delta^{13}C$ land plant biomarker and pollen records from southeast Atlantic continental margin sediments. Geochemistry, Geophysics, Geosystems 7, Q08010.
Rozanski, K., Araguas, L.A., 1995. Spatial and temporal variability of the stable isotope composition of precipitation over the South American continent. Bulletin de l'Institut Français d'Etudes Andines 24, 379–390.
Rozanski, K., Araguás-Araguás, L., Gonfiantini, R., 1993. Isotopic patterns in modern global precipitation. Geophysical Monograph 78, 1–36.
Sachse, D., Radke, J., Gleixner, G., 2004. Hydrogen isotope ratios of recent lacustrine sedimentary *n*-alkanes record modern climate variability. Geochimica et Cosmochimica Acta 68, 4877–4889.
Sachse, D., Radke, J., Gleixner, G., 2006. δD values of individual *n*-alkanes from terrestrial plants along a climatic gradient – implications for the sedimentary biomarker record. Organic Geochemistry 37, 469–483.
Sachse, D., Kahmen, A., Gleixner, G., 2009. Significant seasonal variation in the hydrogen isotopic composition of leaf-wax lipids for two deciduous tree ecosystems (*Fagus sylvativa* and *Acer pseudoplatanus*). Organic Geochemistry 40, 732–742.
Sachse, D., Gleixner, G., Wilkes, H., Kahmen, A., 2010. Leaf wax *n*-alkane δD values of field-grown barley reflect leaf water δD values at the time of leaf formation. Geochimica et Cosmochimica Acta 74, 6741–6750.
Sachse, D., Billault, I., Bowen, G.J., Chikaraishi, Y., Dawson, T.E., Feakins, S.J., Freeman, K.H., Magill, C.R., McInerney, F.A., van der Meer, M.T.J., Polissar, P., Robins, R.J., Sachs, J.P., Schmidt, H.-L., Sessions, A.L., White, J.W.C., West, J.B., Kahmen, A., 2012. Molecular paleohydrology: interpreting the hydrogen-isotopic composition of lipid biomarkers from photosynthesizing organisms. Annual Review of Earth and Planetary Sciences 40, 221–249.
Sauer, P.E., Eglinton, T.I., Hayes, J.M., Schimmelmann, A., Sessions, A.L., 2001. Compound-specific D/H ratios of lipid biomarkers from sediments as a proxy for environmental and climatic conditions. Geochimica et Cosmochimica Acta 65, 213–222.
Schefuss, E., Kuhlmann, H., Mollenhauer, G., Prange, M., Patzold, J., 2011. Forcing of wet phases in southeast Africa over the past 17,000 years. Nature 480, 509–512.
Schellekens, J., Barberá, G.G., Buurman, P., 2013. Potential vegetation markers – analytical pyrolysis of modern plant species representative of Neolithic SE Spain. Journal of Archaeological Science 40, 365–379.
Schulze, E., 1986. Whole-plant responses to drought. Functional Plant Biology 13, 127–141.
Schulze, E.D., Mooney, H.A., Sala, O.E., Jobbagy, E., Buchmann, N., Bauer, G., Canadell, J., Jackson, R.B., Loreti, J., Oesterheld, M., Ehleringer, J.R., 1996. Rooting depth, water availability, and vegetation cover along an aridity gradient in Patagonia. Oecologia 108, 503–511.
Sinninghe Damsté, J.S., Verschuren, D., Ossebaar, J., Blokker, J., van Houten, R., van der Meer, M.T.J., Plessen, B., Schouten, S., 2011. A 25,000-year record of climate-induced changes in lowland vegetation of eastern equatorial Africa revealed by the stable carbon-isotopic composition of fossil plant leaf waxes. Earth and Planetary Science Letters 302, 236–246.
Smith, F.A., Freeman, K.H., 2006. Influence of physiology and climate on δD of leaf wax *n*-alkanes from C_3 and C_4 grasses. Geochimica et Cosmochimica Acta 70, 1172–1187.
Smith, R.M., Martin-Smith, M., 1978. Triterpene methyl ethers in leaf waxes of *Saccharum* and related genera. Phytochemistry 17, 1307–1312.
Stewart, G., Turnbull, M., Schmidt, S., Erskine, P., 1995. ^{13}C natural abundance in plant communities along a rainfall gradient: a biological integrator of water availability. Functional Plant Biology 22, 51–55.
Still, C.J., Powell, R.L., 2010. Continental-scale distributions of vegetation stable carbon isotope ratios. In: West, J.B., Bowen, G.J., Dawson, T.E., Tu, K.P. (Eds.), Isoscapes: Understanding Movement, Pattern, and Process on Earth through Isotope Mapping. Springer, Dordrecht, The Netherlands, pp. 179–193.
Still, C.J., Berry, J.A., Collatz, G.J., DeFries, R.S., 2003. Global distribution of C_3 and C_4 vegetation: carbon cycle implications. Global Biogeochemical Cycles 17, 1006.
Tieszen, L.L., Senyimba, M.M., Imbamba, S.K., Troughton, J.H., 1979. The distribution of C_3 and C_4 grasses and carbon isotope discrimination along an altitudinal and moisture gradient in Kenya. Oecologia 37, 337–350.
Tipple, B.J., Berke, M.A., Doman, C.E., Khachaturyan, S., Ehleringer, J.R., 2013. Leaf-wax *n*-alkanes record the plant–water environment at leaf flush. Proceedings of the National Academy of Sciences of the United States of America 110, 2659–2664.
Vogts, A., Moossen, H., Rommerskirchen, F., Rullkötter, J., 2009. Distribution patterns and stable carbon isotopic composition of alkanes and alkan-1-ols from plant waxes of African rain forest and savanna C_3 species. Organic Geochemistry 40, 1037–1054.
White, F., 1983. The Vegetation of Africa. A descriptive Memoir to Accompagny the UNESCO/AETFAT/UNSO Vegetation Map of Africa. UNESCO, Paris, France.